



# Passive Cooling of Multijunction Concentrator Photovoltaic Solar Cells

H. Zaghloul, M. Emam, M.A. Abdelrahman, M. Fayek.

Department of Mechanical Engineering, Benha University, Egypt

**ABSTRACT.** : solar concentrator photovoltaic (cpv) is a potential solution to provide renewable energy at higher efficiency and less cost. the elevated temperature of the solar cells due to the accumulated heat leads to a decrease in the electricity generation efficiency of the solar cell. the current study aims to enhance the multijunction (mj) solar cell electrical conversion efficiency using a passive cooling technique. three configurations of mj solar cell modules as follows, a mj solar cell module without any heat sink, a mj solar cell module with flat plate fin and a mj solar cell module with straight fins attached to a flat plate base were simulated using acfd software. the effects of the ambient temperature have been studied under the constant solar concentration of 50 suns and wind speed of 1 m/s. the results showed that using a heat sink decreases the maximum solar cell temperature by 43.9% and 50.68% and consequently increases the solar cell efficiency by 4.08% and 4.68% in case of flat plate fin and straight fins attached to a flat plate base respectively compared to the solar cell without any heat sink.

**KEYWORDS:** multijunction solar cells, concentrator photovoltaic, heat sink, straight fins, flat plate fin.

## NOMENCLATURE

Symbols	Description	Symbols	Description
<b>Roman</b>		<b>Greek</b>	
$A$	area	$\alpha$	absorptivity
$c_p$	specific heat capacity	$\beta_{rel}$	relative temperature coefficient
CR	concentration ratio	$\epsilon$	emissivity
$G$	solar irradiance	$\eta$	efficiency
$\dot{q}'''$	heat generation per unit volume	$\rho$	density
$h$	heat transfer coefficient	<b>Subscripts</b>	
$k$	thermal conductivity	<i>ceramic</i>	ceramic layer
$L$	length	<i>cu-lower</i>	lower copper layer
$L_{fin}$	fins length	<i>cu-upper</i>	upper copper layer
$S$	fins spacing	<i>ref</i>	reference
$t$	thickness	<i>sc</i>	solar cell
$T$	Temperature		
$V$	volume		
$v_{wind}$	wind speed		
$W$	width		

## 1. INTRODUCTION

Recently, investments in solar energy have increased significantly as a clean and sustainable source of energy. Hence, a lot of efforts have been made to improve the performance of solar energy and to increase its potential. Hence, concentrator photovoltaic's (CPV) has emerged as one of the potential technologies to provide renewable solar energy at higher efficiency and less cost.

CPV technology includes an optical system that focuses direct sunlight over a large optics area onto a small solar cell as shown in Fig 1. The concentration ratio (CR) is defined as the ratio of optics area to solar cell area and usually referred to as "suns" where one sun equals solar radiation of  $1000 \text{ W/m}^2$ . The concentration of an optic or system of optics can be categorized as low for CR <10 suns, medium for CR 10–100 suns, high for CR 100–1000 suns, or ultra-high for CR >1000[1,2].

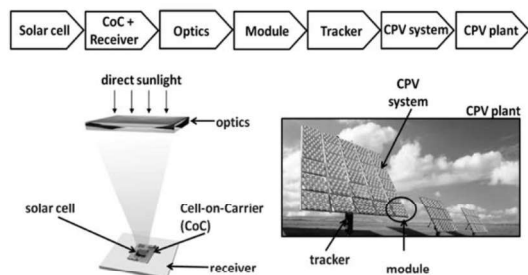


Fig 1. Components and systems of a CPV plant [3].

The CPV technology permits the use of the most efficient cells since the small size of the cell consumes much less semiconductor material. Therefore, CPV replaces expensive semiconductor solar cells with cheaper optics. However, the CPV system needs the usage of high-efficiency solar cells to reduce the lost energy in the form of thermal energy dissipation to be maintained below the maximum operating temperature limit while receiving concentrated solar irradiance. Therefore, a multijunction solar cell made of III-VI materials is typically used in the CPV applications to receive larger concentration ratios [4].

In multi-junction cells, several cell materials with different band gaps are combined in order to maximize the amount of sunlight that can be converted into electricity. Thus, two or more cells are stacked onto each other. The top cell has the highest band gap, in order to absorb and convert the short wavelength (blue) light. Light with

wavelengths longer than the bandgap-wavelength can traverse the top cell and be absorbed in the cells below with lower bandgaps. The bottom cell has the lowest band gap to absorb the long wavelength (red and near infrared) light.

The cooling of the CPV systems has been investigated both numerically and experimentally because of its significance and potential to increase solar energy utilization. Aldossary et al.[5] compared computationally the active cooling of the water channel and passive cooling using heat sink of round pins and straight fins and recommended the active cooling technique for CPV systems of MJ solar cells if they would work in hot atmospheres where the ambient air temperature may reach  $50^\circ\text{C}$  after. Therist is et O'Donovan [6] informed that a single  $10 \times 10 \text{ mm}^2$  needs a heat sink with thermal resistance lower than  $1.4 \text{ }^\circ\text{C/W}$  to maintain the MJ solar cell lower the safe limit of  $80^\circ\text{C}$  for concentration up to 500 suns. Polycrystalline solar cells can reach a concentration ratio of 20 suns with active cooling through micro channels for an ambient air temperature of  $30^\circ\text{C}$  and wind speed of  $1 \text{ m/s}$  as mentioned by Radwan et Ahmed [7]. A more complex configuration which is the flared heat sink is used for concentrator MJ solar cell module. Luo et al. [8] investigated experimentally the effect of various structural parameters on the passive cooling of the MJ solar cell module in CPV systems. Li et al.[9] studied numerically the performance of the natural convection for a flared heat sink used for  $1 \text{ cm}^2$  ceramic with heat generation of  $31 \text{ W}$  used as heat source the same as MJ solar cell at an ambient temperature of  $27^\circ\text{C}$ .

The passive cooling for MJ solar cells at a medium concentration ratios not well covered in the literature. The straight fins heat sink offers a simple configuration for passive cooling. The passive cooling is favored over active cooling as it does not need maintenance and no pumping power is deducted from solar cell output power. The current study aims to simulate the performance of the multijunction concentrated solar cell at different ambient temperatures under the medium solar concentration of 50 suns and wind speed of  $1 \text{ m/s}$ . The study carried out on the following three cases: uncooled MJ solar cell, natural cooling of MJ solar cell using a flat plate

as a heat sink, and natural cooling using straight fins attached to a flat plate base as a heat sink.

## 2. PHYSICAL MODEL

In this work, a triple-junction solar cell created from three stacked cells of III-VI materials of GaInP, GaInAs, and Ge substrate. Since the GaInP and GaInAs cells are much smaller than the Germanium substrate, the solar cell can be thermally modeled as one cell of Germanium as confirmed by [10]. The cell is attached to a circuit board that consists of three layers; the upper copper layer, the middle Al<sub>2</sub>O<sub>3</sub> ceramic layer, and the lower copper layer as illustrated in Fig 2a. The data of this module are taken from AZUR SPACE datasheet of the latest MJ solar cell module type 3C44A [11]. Different types of heat sinks are simulated in the current work. The first configuration is the MJ solar cell module without any heat sink as indicated in Fig 2a. The second configuration includes the MJ solar cell module placed on a flat base plate of aluminum as shown in Fig 2b. The third configuration uses straight fins of aluminum that are attached to the flat plate as illustrated in Fig 2c. The dimensions of the assembly are listed in Table 1.

Table 1. Multijunction solar cell module with heat sink dimensions in mm.

Layer	Length (L)	Width (W)	Thickness (t)
Solar cell	10	10	0.19
Upper copper	27.6	25.6	0.25
Al <sub>2</sub> O <sub>3</sub> ceramic	31.6	29.6	0.32
Lower copper	29.6	27.6	0.25
Flat plate base	100	100	2
Straight fins	75	100	2

Table 2. Properties of the materials of the MJ solar cell module.

Material	$k$ (W /m <sup>2</sup> K)	$c_p$ (J /kgK)	$\rho$ (kg /m <sup>3</sup> )	$\epsilon$
Germanium	60	320	5323	0.9
Copper	400	385	8700	0.05
Al <sub>2</sub> O <sub>3</sub> ceramic	30	900	3900	0.75
Aluminum	202.6	871	2719	0.9

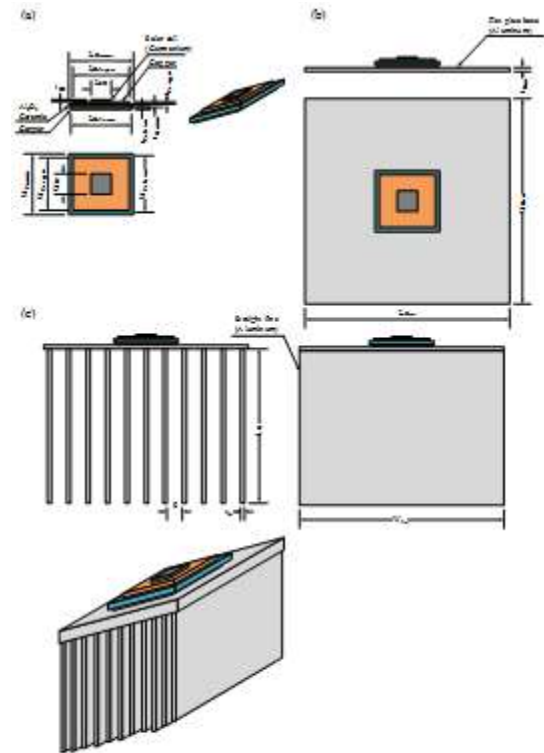


Fig 2. (a) the MJ solar cell module without a heat sink, (b) the MJ solar cell with flat plate fin, (c) the MJ solar cell with straight fins attached to a flat plate base.

## 3. NUMERICAL SOLUTION

The geometry of the physical model described in the previous section is created on the design modeler. Then mesh is created using the multi-blocking technique to yield a structured mesh. In the solver, the energy equation is activated. The materials properties in

Table 2 are applied for each layer of the model.

For boundary conditions, adiabatic sides are applied. For top surfaces, mixed radiation and convection heat transfer with the ambient air is applied. For bottom surfaces, only convection is considered while radiation losses are neglected. The source term is only valid for the solar cell layer and it is calculated as follows [12]:

$$q_{sc}''' = \frac{(1 - \eta_{sc}) \cdot CR \cdot G \cdot \alpha_{sc} \cdot A_{sc}}{V_{sc}} \quad (1)$$

where  $(CR \times G)$  represents the concentrated incident solar irradiance on the solar cell surface area,  $\alpha_{sc}$  is the absorptivity of the solar cell which is taken as 0.9.  $A_{sc}$  and  $V_{sc}$  are the top surface area and the volume of the solar cell layer respectively.  $\eta_{sc}$  is the solar cell efficiency given as:

$$\eta_{sc} = \eta_{ref} (1 + \beta_{rel} (T_{sc} - T_{ref})) \quad (2)$$

where the reference temperature  $T_{ref} = 25^\circ\text{C}$ , the reference solar cell efficiency  $\eta_{ref} = 42\%$  and the solar cell relative efficiency temperature

coefficient  $\beta_{rel} = -0.106\%/^{\circ}\text{C}$  [11]. The convection heat transfer coefficient is dependent on the wind velocity ( $v_{wind}$ ) as evaluated from the following equation [5]:

$$h = 5.82 + 4.07 v_{wind} \quad (3)$$

The convergence criterion has been set to reduce the scaled residuals of the energy to be below the value of  $10^{-16}$ .

### 3.1 Mesh independence test

Mesh independence test is performed for each configuration in the present study to ensure that the results did not depend on the number of elements. The mesh independence test is performed for MJ solar cell without heat sink at high CR. The maximum solar cell temperature is calculated for every number of mesh cells to determine at which number of the mesh cells the maximum cell temperature would be independent of the number of cells increase. The results of the test shown in Fig 3, indicate that there is no significant change in the maximum solar cell temperature with a further increase in the number of mesh cells after reaching 737,140 cells. Therefore, it is chosen for the current model.

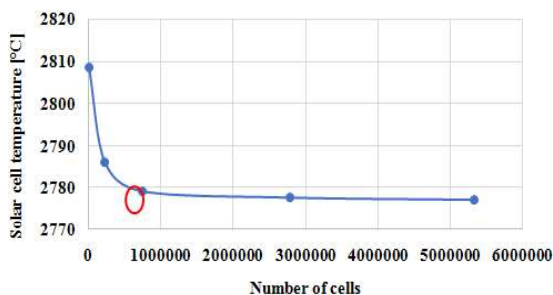


Fig 3. Mesh independence test of MJ solar cell module with a straight fins heat sink

### 3.2 Model validation

The model is validated by comparing the results found in the literature with the data yielded from the current developed thermal model. Fig 4 compares the temperature contours of the MJ solar cell module without heat sink as provided from the current model and the results found in the numerical simulation of [13]. In this case, the solar cell module is exposed to a concentration ratio  $CR = 50$  suns, at an ambient temperature of  $25^{\circ}\text{C}$  and a wind speed of  $1\text{m/s}$ . The temperature contours of the current model are in good agreement with the numerical results of [13] as illustrated in Fig 4.

## 4. RESULTS AND DISCUSSION

The variation of average solar cell temperature with the ambient air temperature at solar concentration of 50 suns and wind speed of  $1\text{m/s}$

is illustrated in Fig 5a. It can be seen that by increasing the ambient temperature from  $25^{\circ}\text{C}$  to  $40^{\circ}\text{C}$ , the solar cell average surface temperature increases from  $70^{\circ}\text{C}$  to  $85.6^{\circ}\text{C}$  with a rate of  $1.0388^{\circ}\text{C}$  increase in solar cell temperature for every  $1^{\circ}\text{C}$  increase in the ambient temperature. Due to passive cooling using the two types of fins, the solar cell average temperatures decrease by  $37.3^{\circ}\text{C}$  and  $43^{\circ}\text{C}$  on average in case of MJ solar cell with flat plate fin and MJ solar cell with straight fins respectively.

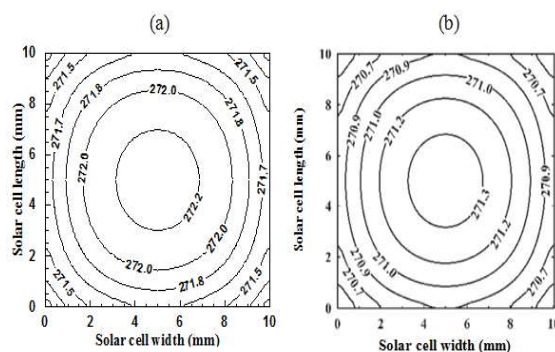


Fig 4. Temperature ( $^{\circ}\text{C}$ ) contours of the solar cell surface area under  $CR = 50$  without a heat sink.

(a) Temperature contours of the current model,  
(b) Temperature contours of [13].

The solar cell electrical conversion efficiency with ambient of air temperature at solar concentration of 50 suns and wind speed of  $1\text{m/s}$  is calculated using equation(2) and plotted as shown in Fig 5b. From the figure, it can be observed that the solar cell efficiency decreases with increases of ambient temperature from  $25^{\circ}\text{C}$  to  $40^{\circ}\text{C}$ , as it deteriorates by a rate of  $0.046\%/^{\circ}\text{C}$ . The reduction in solar cell surface temperature is reflected in the electrical conversion efficiency as the efficiency increases due to cooling by  $4.26\%$  and  $4.91\%$  on average in case of MJ solar cell with flat plate fin and MJ solar cell with straight fins attached to a flat plate base respectively.

Fig 6 illustrates the effect of each heat sink configuration on the temperature distribution. The temperature distribution is examined at the cross-section view in the half-width of the solar cell. Fig 6a indicates that the maximum temperature in the assembly at the center of the solar cell with a temperature of  $42.3^{\circ}\text{C}$  in case of using straight fins heat sink. While the maximum solar cell temperature was  $48.2^{\circ}\text{C}$  and  $85.8^{\circ}\text{C}$  for flat plate heat sink and without heat sink configurations as shown in Fig 6b and Fig 6c respectively.

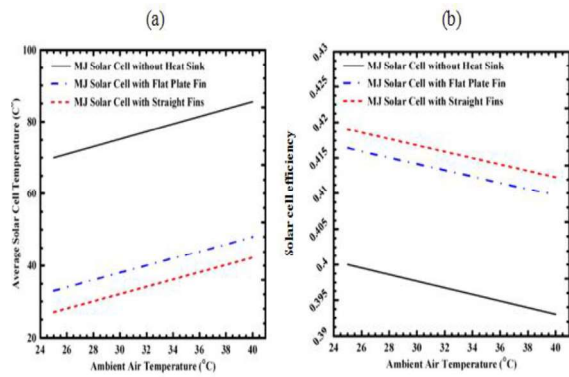


Fig 5. Ambient air temperature variation effect on  
(a) average solar cell temperature,  
(b) solar cell efficiency.

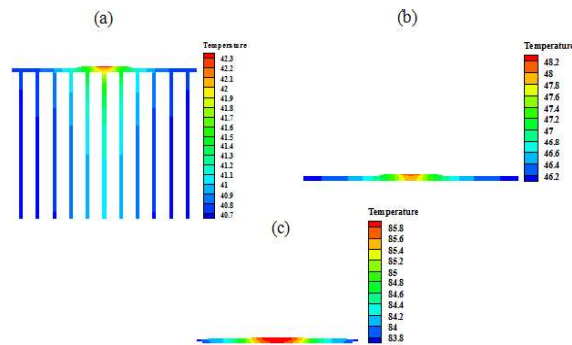


Fig 6. Temperature distribution in the mid-cross-section of: (a) the MJ solar cell with straight fins heat sink, (b) the MJ solar cell with flat plate fin, (c) the MJ solar cell without a heat sink.

## 5. CONCLUSIONS

This study investigated numerically the effect of using heat sink for passive cooling of multijunction solar cells. Flat plate fin and straight fins were studied at different ambient air temperatures under constant solar concentration ratio of 50 suns and wind speed of 1 m/s. The solar cell average temperatures decrease by 37.56°C and 43.37 °C on average in case of MJ solar cell with flat plate fin and MJ solar cell with straight fins respectively. Under the same conditions, the usage of the flat plate fin improves the electrical conversion efficiency by 4.08% while the straight fins heat sink improves the MJ solar cell efficiency by 4.68% in reference to the efficiency of the MJ solar cell without any heat sink. Thus, at low concentration ratios, the passive cooling is suitable for the satisfactory operation of the concentrator MJ solar cells.

## 6. REFERENCES

- [1] Sripadmanabhan Indira S, Vaithilingam CA, Chong K-K, Saidur R, Faizal M, Abubakar S, et al. A review on various configurations of hybrid concentrator photovoltaic and thermoelectric generator system. *Sol Energy* 2020;201:122–48. doi:10.1016/j.solener.2020.02.090.
- [2] Pérez-Higueras P, Fernández EF. *High Concentrator Photovoltaics*. vol. 130. Cham: Springer International Publishing; 2015. doi:10.1007/978-3-319-15039-0.
- [3] Algora C, Rey-Stolle I, editors. *Handbook of Concentrator Photovoltaic Technology*. Chichester, West Sussex: John Wiley & Sons, Ltd; 2016. doi:10.1002/9781118755655.
- [4] Kurtz S, Geisz J. Multijunction solar cells for conversion of concentrated sunlight to electricity. *Opt Express* 2010;18:A73. doi:10.1364/oe.18.000a73.
- [5] Aldossary A, Mahmoud S, Al-Dadah R. Technical feasibility study of passive and active cooling for concentrator PV in harsh environment. *Appl Therm Eng* 2016;100:490–500. doi:10.1016/j.applthermaleng.2016.02.023.
- [6] Theristis M, O'Donovan TS. Electrical-thermal analysis of III-V triple-junction solar cells under variable spectra and ambient temperatures. *Sol Energy* 2015;118:533–46. doi:10.1016/j.solener.2015.06.003.
- [7] Radwan A, Ahmed M. The influence of microchannel heat sink configurations on the performance of low concentrator photovoltaic systems. *Appl Energy* 2017;206:594–611. doi:10.1016/j.apenergy.2017.08.202.
- [8] Luo Q, Li P, Cai L, Chen X, Yan H, Zhu H, et al. Experimental investigation on the heat dissipation performance of flared-fin heat sinks for concentration photovoltaic modules. *Appl Therm Eng* 2019;157:113666. doi:10.1016/j.applthermaleng.2019.04.076.
- [9] Li P, Yan H, Luo Q, Liang D, Li P. Numerical study on natural convection heat dissipation of flared fin heat sink for high concentrating photovoltaic module cooling. *Energy Sources*,

Part A Recover Util Environ Eff 2019;41:573–83. doi:10.1080/15567036.2018.1520341.

- [10] Chou TL, Shih ZH, Hong HF, Han CN, Chiang KN. Thermal performance assessment and validation of high-concentration photovoltaic solar cell module. *IEEE Trans Components, Packag Manuf Technol* 2012;2:578–86. doi:10.1109/TCPMT.2011.2181165.
- [11] Azure Space Solar Power GMBH. Enhanced Fresnel Assembly - EFA Type: 3C42A – with 10x10mm<sup>2</sup> CPV TJ Solar Cell Application: Concentrating Photovoltaic (CPV) Modules 2014:0–4.
- [12] Abo-Zahhad EM, Ookawara S, Radwan A, El-Shazly AH, El-Kady MF, Esmail MFC. Performance, limits, and thermal stress analysis of high concentrator multijunction solar cell under passive cooling conditions. *Appl Therm Eng* 2020;164:114497. doi:10.1016/j.applthermaleng.2019.114497.
- [13] Abo-Zahhad EM, Ookawara S, Radwan A, El-Shazly AH, ElKady MF. Thermal and structure analyses of high concentrator solar cell under confined jet impingement cooling. *Energy Convers Manag* 2018;176:39–54. doi:10.1016/j.enconman.2018.09.005.